ARTICLES

Molecular design of strong single-wall carbon nanotube/polyelectrolyte multilayer composites

ARIF A. MAMEDOV[1], NICHOLAS A. KOTOV*[1], MAURIZIO PRATO[2], DIRK M. GULDI[3], JAMES P. WICKSTED[4] AND ANDREAS HIRSCH[5]

[1]Chemistry Department, Oklahoma State University, Stillwater, Oklahoma 74078, USA
[2]Dipartimento di Scienze Farmaceutiche, Università di Trieste, Piazzale Europa, 1, 34127 Trieste, Italy
[3]Radiation Laboratory, University of Notre Dame, Notre Dame, Indiana 46556, USA
[4]Department of Physics, Center for Sensors and Sensor Technologies, Oklahoma State University, Stillwater, Oklahoma 74078, USA
[5]Institut für Organische Chemie, Lehrstuhl II, Universität Erlangen-Nürnberg, Henkestraße 42, D-91054 Erlangen, Germany
*e-mail: kotov@okstate.edu

The mechanical failure of hybrid materials made from polymers and single-wall carbon nanotubes (SWNT) is primarily attributed to poor matrix–SWNT connectivity and severe phase segregation. Both problems can be successfully mitigated when the SWNT composite is made following the protocol of layer-by-layer assembly. This deposition technique prevents phase segregation of the polymer/SWNT binary system, and after subsequent crosslinking, the nanometre-scale uniform composite with SWNT loading as high as 50 wt% can be obtained. The free-standing SWNT/polyelectrolyte membranes delaminated from the substrate were found to be exceptionally strong with a tensile strength approaching that of hard ceramics. Because of the lightweight nature of SWNT composites, the prepared free-standing membranes can serve as components for a variety of long-lifetime devices.

Exceptional mechanical properties of single-wall carbon nanotubes (SWNT)[1–6] have prompted intensive studies of SWNT composites. However, the present composites have shown only a moderate strength enhancement when compared with other hybrid materials[7–9]. Although substantial advances have been made[10], mechanical properties of SWNT-doped polymers are noticeably below their highly anticipated potential. Pristine SWNTs are well known for poor solubilization, which leads to phase segregation of composites. Severe structural inhomogeneities result in the premature failure of the hybrid SWNT/polymer materials. The connectivity with, and uniform distribution within the matrix are essential structural requirements for the strong SWNT composites[11–13]. Here we show that a new processing approach based on sequential layering of chemically modified nanotubes and polyelectrolytes can greatly diminish the phase segregation, and render SWNT composites highly homogeneous. Combined with chemical crosslinking, this processing leads to drastically improved mechanical properties. The tensile strength of the composites is several times higher than that of SWNT composites made by mixing, and approaches values seen for hard ceramics. The universality of the layering approach is applicable to a wide range of functional materials. Successful incorporation of SWNT into a variety of composites should be possible, imparting them with the required mechanical properties.

SWNT composites are typically prepared by blending, *in situ* polymerization and extrusion. After extensive surface modification, such as grafting or polymer wrapping[12–14], the phase segregation from a macromolecular matrix is smaller than for pristine SWNT, but still remains high owing to vastly different molecular mobilities of both components. For that reason, most common loadings of nanotubes in the polymer matrix are within the 1–15 wt% range, whereas more than 50% of the SWNT content is needed for materials with special mechanical performance without compromising the homogeneity of the composite at the nanometre level. The phase segregation between dissimilar
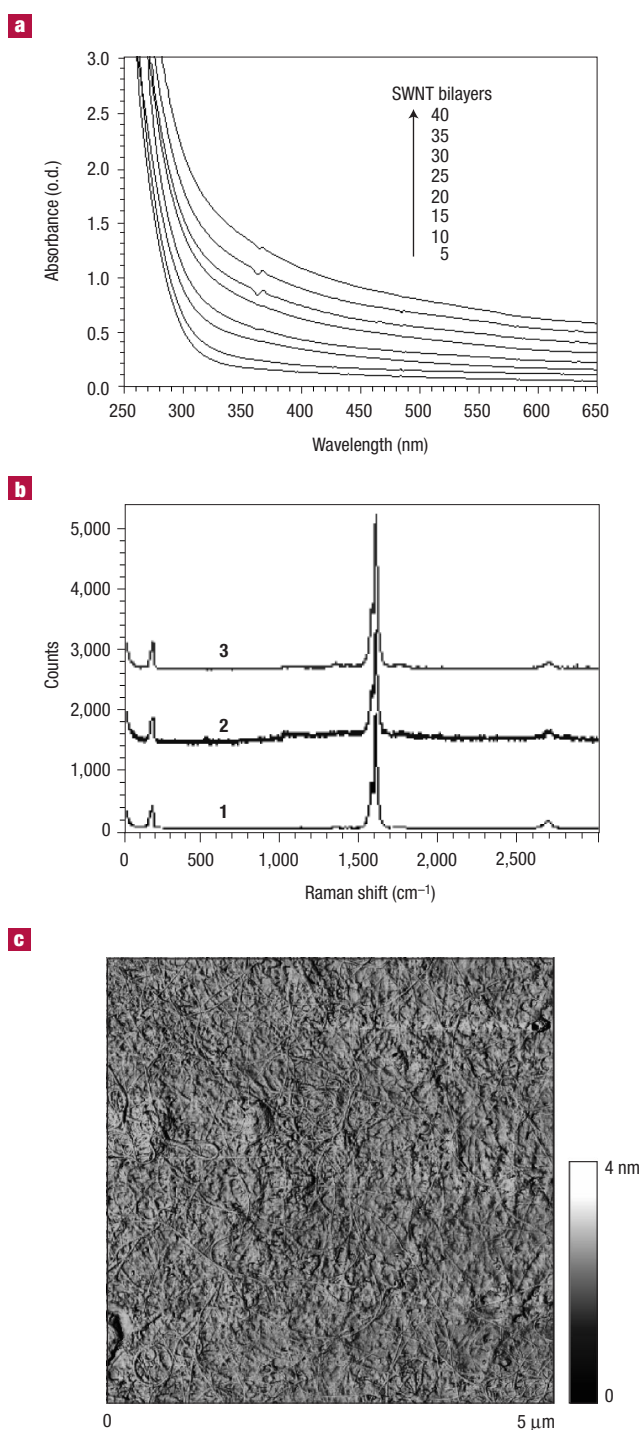
Figure 1 Structural characterization of SWNT multilayers. a, Sequential ultraviolet–visible optical density (o.d.) spectra of a glass substrate in the course of the LBL deposition of SWNT. The spectra were taken for a total number of (PEI/SWNT) bilayers indicated in the graph. **b**, Raman scattering spectra of SWNT dispersion (1), LBL film on a glass substrate (2), and free-standing film (3). **c**, Tapping-mode AFM image (DI, Multimode IIIA) of a silicon wafer bearing (PEI/PAA)(PEI/SWNT)$_5$.

materials can be circumvented by applying a new deposition technique often called layer-by-layer assembly (LBL)[15]. This technique is based on the alternating adsorption of monolayers of individual components attracted to each other by electrostatic and van der Waals interactions. The immobilization of the macromolecular compounds and strong interdigitation of the nanometre-thick film allows for the close-to-perfect molecular blending of the components[16–17].

The SWNT/polyelectrolyte composites produced in this study were assembled on to a solid support by alternate dipping of a solid substrate (glass slides, silicon wafers) into dispersions of SWNT and polyelectrolyte solutions[18,19]. The individual assembly steps, that is, adsorption of SWNT and polyelectrolyte monolayers, were separated by rinsing steps to remove the excess of assembling materials. When the LBL procedure was complete, the multilayer films were lifted off the substrate to obtain uniform free-standing membranes that can be handled as regular composites[20]. Such films make straightforward testing of their mechanical properties possible.

SWNTs were manufactured by laser vapourization of carbon rods doped with Co, Ni and FeS in an atmosphere of Ar:H$_2$. A suspension of SWNT raw material was refluxed in 65% HNO$_3$ and subsequently purified by centrifugation. Supplemented by sonication, this treatment results in the partial oxidation of about 5% of the total number of carbon atoms both in the caps and walls of SWNT[21]. The presence of carboxylic acid groups allows the preparation of metastable SWNT dispersions after 1 min of sonication in deionized water without any additional surfactant. These negatively charged SWNTs with a zeta-potential of –0.08 V can be assembled layer-by-layer with positively charged polyelectrolyte, such as branched poly(ethyleneimine) (PEI, Aldrich), of molecular weight $M_w = 70,000$. Because the overall negative charge of the SWNT used here was fairly small, after every fifth deposition cycle, a layer of SWNT was replaced with a layer of poly(acrylic acid) (PAA, Aldrich), $M_w = 450,000$. These additional layers improve the linearity of the deposition process, and present a convenient chemical anchor for subsequent chemical modification. For the same reasons, a single PEI/PAA bilayer was deposited on a bare glass or silicon substrate before the SWNT assembly. All solutions were made in 18 MOhm deionized water. Deionized water was also used for rinsing at pH 8.5 adjusted by NaOH. Wafers/glass slides were cleaned in piranha solution (a 1:3 mixture of 30% H$_2$O$_2$ and concentrated H$_2$SO$_4$; note that this mixture is dangerous as it violently reacts with organics), rinsed with deionized water, sonicated for 15 min and again thoroughly rinsed with deionized water. They were then coated with a precursor layer: PEI (10 min) + PAA (15 min, pH 3), followed by the deposition of (PEI/SWNT)$_5$. The 1% PEI solution was at pH 8.5; 1% PAA solution was at pH 6 (pH 3 for wafer coating); SWNT solution was at pH 6.8. The layer sequence of (PEI/PAA)(PEI/SWNT)$_5$ was repeated until the desirable thickness was obtained. Exposure times of 10 and 60 min were used for polyelectrolytes and SWNT baths, respectively. The assembly conditions of the entire procedure (such as pH, ionic strength and concentrations) were optimized so that the dipping cycles could be repeated as many times as needed with linear growth of the multilayers (Fig. 1a). This enables the preparation of films with any desirable thickness and architecture tailored to different applications. Multilayer stacks with a cumulative structure of ((PEI/PAA)(PEI/SWNT)$_5$)$_6$ and ((PEI/PAA)(PEI/SWNT)$_5$)$_8$ containing 30 and 40 (PEI/SWNT) bilayers, respectively, were typically used in this study.

Similarly to other polyelectrolyte LBL systems[15], an interdigitated layer of SWNT is deposited in each deposition cycle. The final morphology of the multilayers can be described as a mixture of individual carbon nanotubes and their 4–9 nm bundles intricately interwoven together in a fine fabric (Fig. 1c). Two important structural characteristics should be pointed out. SWNT uniformly cover the entire surface of the substrate without any evidence of phase separation. Also, in our experiments, the presence of oxidized flat graphite sheets, and other forms of carbon colloids, was minimal. Both these factors contributed to the mechanical properties of the composites. The quality of the nanotube
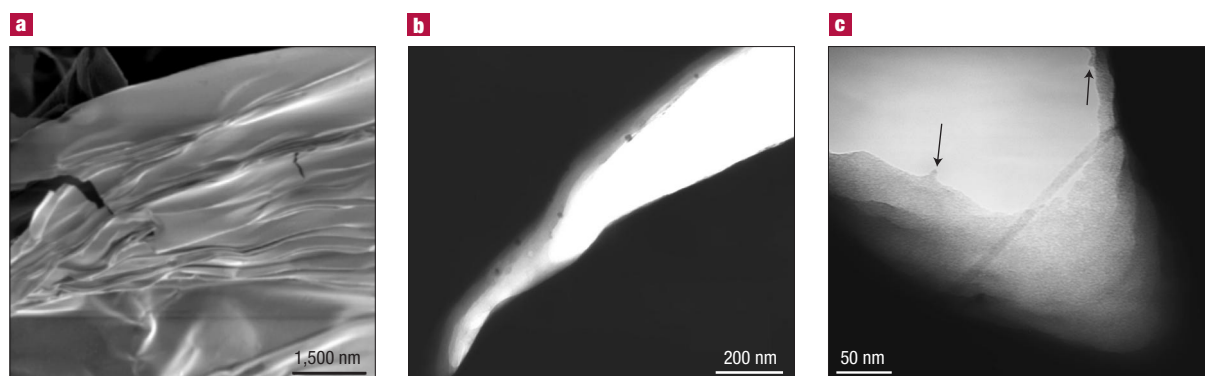
Figure 2 Electron microscopy of the rupture region in SWNT multilayers. **a**, SEM image of the surface and broken edges of ((PEI/PAA)(PEI/SWNT)$_5$)$_8$. **b**, and **c**, TEM images of ruptured areas of the free-standing films. The arrows indicate the possible positions of the stubs of the broken nanotube bundles. They were identified as such because the diameter of both of them is similar to that of the actual SWNT bundle bridging the gap, and their mutual positioning presents an almost perfect match with the expected location of the ends of a bundle broken during gap opening.

material was also assessed by Raman spectroscopy (Fig. 1b). Raman measurements were performed in a backscattering configuration with a 50 mW laser light at 514.5 nm incident on the samples. The characteristic Raman peaks for SWNTs, for example, the radial breathing mode (RBM) at ~182 cm^{-1}, in which carban atoms are undergoing radial displacement, and the tangential C–C stretching modes located at ~1560 cm^{-1} (G$_1$ mode) and ~1583 cm^{-1} (G$_2$ mode), which result from the splitting of the E_{2g} stretching mode in graphite, were very sharp and narrow indicating the high uniformity of the SWNT and low level of impurities present in the films. A barely visible peak at ~1340 cm^{-1} (D mode) resulting from disordered-inducing Raman

scattering from sp^2 carbons. Using the correlation between the frequency of the radial breathing mode, v, and the SWNT diameter, d, expressed as $d = 223.75/v$ (ref. 22), a value of $d = 1.2$ nm was obtained, which is in a good agreement with the SWNT diameters obtained from AFM (atomic force microscopy) images of many individual nanotubes. From these images, the length of the nanotubes was estimated to be 2–7 μm.

PEI was used as the LBL partner of SWNT because of the terminal –NH$_2$ and backbone –NH– groups in the main chain and branches, which are suitable for the subsequent chemical modification of the composite[23]. The PEI chains can be either crosslinked with each other or with carboxyl groups on SWNT and PAA. Chemical stitching increases the connectivity
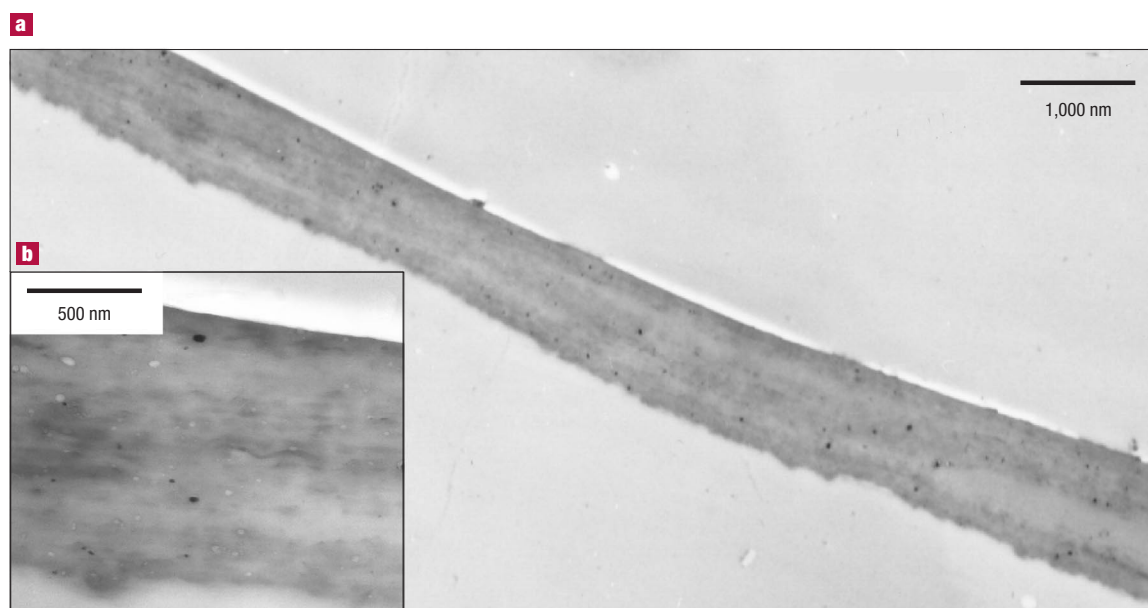

Figure 3 Examination by TEM of the homogeneity of the SWNT LBL film. **a**, Survey and **b**, close-up TEM images of SWNT film cross-sections. The top and bottom sides of the film are slightly different in roughness: the one that was adjacent to the flat substrate is smoother than the 'growth' surface of the film.
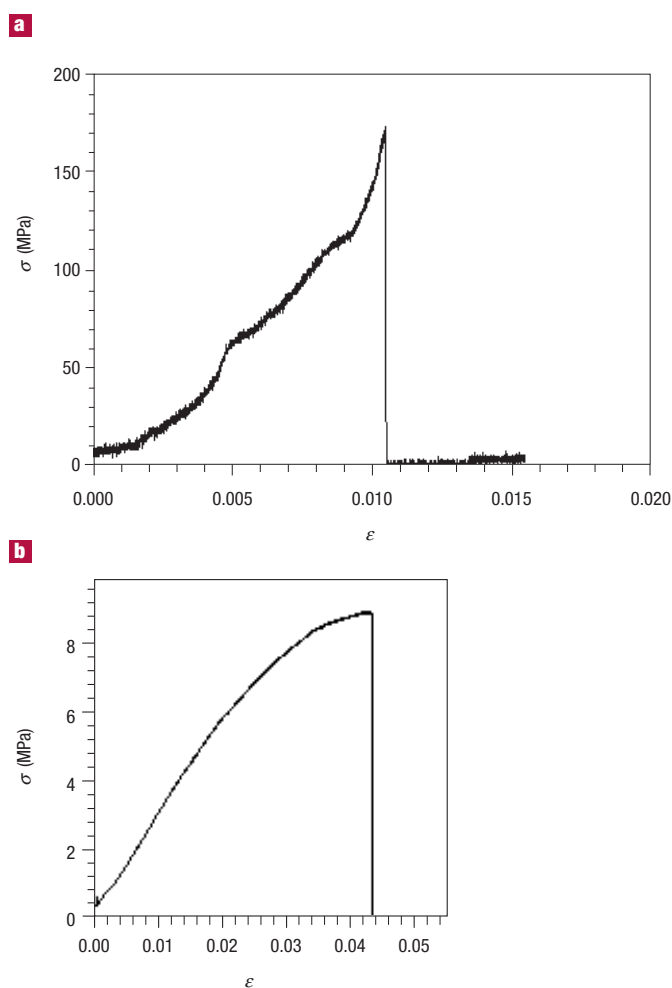
Figure 4 Typical tensile strength curves of the SWNT LBL films. Stress (σ)–strain (ε) dependence for: **a**, ((PEI/PAA)(PEI/SWNT)$_5$)$_8$, and **b**, a similar free-standing multilayer film made solely from polyelectrolytes (PEI/PAA)$_{40}$. The dependence of the mechanical properties of the SWNT LBL composites on humidity was tested in the range of relative humidity of 30–100%, at a temperature of 298 °C, and was found to be negligible.

Note that a minor part of these groups is probably utilized at the moment, because of the relatively low temperature of amide bond crosslinking step.

The mechanical properties of the LBL-assembled SWNT thin films were studied in their free-standing form, which was prepared by the chemical delamination from the substrate[20]. SWNT multilayers were separated from the silicon wafers by immersion into 0.5% aqueous hydrofluoric acid for 3 min. The Raman scattering spectrum of the separated film is almost identical to that of the supported film and original nanotubes (Fig. 1b), demonstrating that the structure of SWNT remains mostly unaltered during the crosslinking and delamination. The breathing-mode frequency shifts from 183 cm^{-1} in the assembled film to 181 cm^{-1} in the crosslinked self-standing films, which indicates a small compression of the tube diameters.

The delaminated thin films (Fig. 2a), can be easily handled in a variety of ways. They can be made of any desirable size or shape determined only by the dimensions of the substrate. The films that we routinely prepare in this study were 1 cm by 3 cm. Assemblies with a structure of ((PEI/PAA)(PEI/SWNT)$_5$)$_6$ and ((PEI/PAA)(PEI/SWNT)$_5$)$_8$ displayed an SWNT content of 50 ± 5 wt% as calculated from carbon and nitrogen energy dispersive X-ray analysis peak integrals. Previously reported composites made with modified SWNT revealed strong inhomogeneities[8,9] even at SWNT loadings as low as 6–8% wt%. The cross-sectional images of the free-standing film (Fig. 3a,b) clearly demonstrates the absence of micrometre-scale inhomogeneities, although the occasional inclusion of round 30–60 nm particles can be seen (these are possibly dust). The slight variations in the grey-scale contrast between different strata show the actual variations in SWNT distribution within the sample. They originate from small deviations in SWNT adsorption conditions, such as dispersion concentration and pH, during the build-up procedure. In scanning electron microscopy (SEM), the surface of the sample also appears smooth and continuous (Fig. 2a). Typically, the separation of single/multiwall carbon nanotubes and their bundles in mixed polymer composites can be observed as whiskers clearly visible in images from transmission electron microscopy (TEM) and SEM[4,25]. TEM examination of the initial stages of rupturing showed that virtually no fibre pullout occurs in the LBL multilayers (Fig. 2b). This can be contrasted by extensive nanotube pullout reported before by several groups[4,25]. For many TEM images obtained in different areas of the self-standing films, we were able to observe only one SWNT bundle bridging the break region (Fig. 2c). The same image also shows two broken carbon fibre stubs imbedded in the walls of the crack (marked by arrows in Fig. 2c). Scanning and transmission electron microscopy results indicate the efficient load transfer in the LBL composite.

The mechanical properties of the layered composites were tested on a custom-made thin-film tensile strength tester (McAllister) recording the displacement and applied force by using pieces cut from ((PEI/PAA)(PEI/SWNT)$_5$)$_6$ and ((PEI/PAA)(PEI/SWNT)$_5$)$_8$ free-standing films. The tester was calibrated on similar pieces made from cellulose acetate membranes and nylon threads. ((PEI/PAA)(PEI/SWNT)$_5$)$_6$ and ((PEI/PAA)(PEI/SWNT)$_5$)$_8$ samples had an average thickness, measured by TEM, of 0.75 and 1.0 μm respectively. Their typical stress (δ) versus strain (ε) curves differed quite markedly from stretching curves seen previously for SWNT composites[10] and for LBL films made solely from polyelectrolytes, (PEI/PAA)$_{40}$, obtained by the same assembly procedure (Fig. 4b). They displayed a characteristic wave-like pattern, a gradual increase of the $d\delta/d\varepsilon$ derivative, and the complete absence of the plateau region for high strains corresponding to plastic deformations (Fig. 4a). The latter correlates well with the enhanced connectivity of SWNT with the polymer matrix (Fig. 2). Other stretching features indicate the reorganization of the layered composite under stress. A process similar to the sequential breakage of crosslinked parts of coiled molecules (see AFM image in Fig. 1) observed in natural nanocomposites, such as seashells and bones[26,27], is likely to be responsible for the wave-like pattern and the increase of the slope of the stretching curve. Considering the complexity

of the polyelectrolyte matrix with SWNT, and therefore the load transfer in the composite[13]. Here we used the combination of both modification pathways. Partial covalent SWNT–PEI–PAA crosslinking was achieved by heating the films to 120 °C after the deposition of each layer, resulting in amide bonds between a variety of protonated and non-protonated functional groups of PEI, PAA and SWNT, which complemented the intrinsic ionic crosslinking of the LBL films[24]. Subsequently, the film was crosslinked in 0.5% glutaraldehyde (OCHCH$_2$CH$_2$CH$_2$CHO) solution in phosphonate buffer (0.054 M Na$_2$HPO$_4$, 0.013 M NaH$_2$PO$_4$, pH 7.4) for 1 h at room temperature. To remove unreacted glutaraldehyde, the film was rinsed with tap water for 3 × 10 minutes. and then with deionized water for the same period. This reaction produces a tight network of polymeric chains and nanotubes connected by dialdehyde linkages. It was found that if only 1% of all carbon atoms of SWNT are chemically bonded to the polymer matrix, such crosslinking drastically increases the sheer between them by an order of magnitude[13]. Therefore, a 5% density of –COOH groups on the SWNT surface described above should be sufficient to obtain good connectivity with the polyelectrolyte matrix.

of the deformation process, the assessment of elastic and inelastic behaviour in each part of the curve will be possible by detailed microscopy investigation. Meanwhile, the values of $d\delta/d\varepsilon$ exceeding 35 GPa should be noted.

The comparison with stretching curves for polyelectrolytes (Fig. 4b) shows that the incorporation of nanotubes in the LBL structure resulted in the transfer of the SWNT strength to the entire assembly. The stretching curves of the SWNT multilayers display a clear break point. The ultimate tensile strength, T, was found to be 220 ± 40 MPa with some readings as high as 325 MPa. This is several orders of magnitude greater than the tensile strength of strong industrial plastics[28], which have T values of 20–66 MPa. It is also substantially higher than the tensile strength of carbon fibre composites made by mixing: the T value of polypropylene filled with 50 vol.% carbon fibres is 53 MPa (ref. 29). A recent study[10] on SWNT/poly(vinylalcohol) ribbons with axially aligned nanotubes reported a T of 150 MPa. The T values obtained for SWNT LBL films are, in fact, close to those of ultrahard ceramics and cermets[28] such as tungsten monocarbide, $T = 340$ MPa, silicon monocarbide, $T = 300$ MPa, and tantalum monocarbide, $T = 290$ MPa. Such strength and failure strain, greater than in cermets (>1% in SWNT LBL versus 0.2–0.6% in carbides), displayed by an organic composite is quite remarkable.

The T values of single carbon nanotubes was experimentally determined to be between 13 and 50 GPa[25,30]. The lower values obtained for the SWNT multilayers should be mainly attributed to the contribution of polyelectrolytes and some uncertainty in the actual cross-section area at the breakpoint, and a degree of crosslinking. The mixing law predicts that a polyelectrolyte matrix with $T = 9$ MPa makes a negligible contribution to the strength of the composite, although taking about 50% of its volume fraction. (For SWNT $d = 1.14$ g cm^{-3}. Because the density of the polyelectrolytes used for the preparation of the multilayers—PDDA $d = 1.04$ g cm^{-3}, PAA $d = 1.14$ g cm^{-3}—is almost the same as d of SWNT, the volume fraction of nanotubes in the composite can be considered to be equal to the mass fraction). Additionally, the decrease of the mechanical strength of the nanotubes in the process of ionic functionalization (estimated to be 15%)[31] is also a factor affecting the strength of these composites. These issues are pointed out as a means of further optimization of the multilayers. Tuning of their molecular structure and composition should lead to vast improvement of their mechanical properties, which could possibly approach those of pristine carbon nanotubes.

It is also interesting to compare the T values for SWNT composite films with those obtained for other LBL films made with other inorganic components such as montmorillonite platelets, M, and nanoparticles, NP, for example 8–10 nm magnetite nanoparticles. The free-standing films (PDDA/NP)$_{40}$ and (PDDA/NP/PDDA/M)$_{40}$ prepared as described elsewhere[20] revealed T equal to 40 MPa and 72 MPa, respectively. In conjunction with the T data in Fig. 4, it can be concluded that inorganic or SWNT components act as a molecular armour in the layered composites, significantly reinforcing them. The molecular organization of the material made possible the transfer of a part of their strength to the entire assembly.

The high structural homogeneity and interconnectivity of the structural components of the LBL films combined with high SWNT loading leads to a significant increase in the strength of SWNT composites. The described technique minimizes the structural defects originating from phase segregation, and opens up possibilities for the molecular design of layered hybrid structural materials from different polymers and other nanoscale building blocks. The prepared free-standing membranes can serve as a unique component for a diverse variety of long-lifetime devices including elements of a space station and advanced prostheses.

References

1. Wong, E. W., Sheehan, P. E. & Lieber, C. M. Nanobeam mechanics: elasticity, strength, and toughness of nanorods and nanotubes. *Science* **277**, 1971–1975 (1997).
2. Popov, V. N., Van Doren, V. E. & Balkanski, M. Elastic properties of single-walled carbon nanotubes. *Phys. Rev. B* **61**, 3078–3084 (2000).
3. Baughman, R. H. *et al.* Carbon nanotube actuators. *Science* **284**, 1340–1344 (1999).
4. Qian, D., Dickey, E. C., Andrews, R. & Rantell, T. Load transfer and deformation mechanisms in carbon nanotube-polystyrene composites. *Appl. Phys. Lett.* **76**, 2868–2870 (2000).
5. Yu, M. F. *et al.* Strength and breaking mechanism of multiwalled carbon nanotubes under tensile load. *Science* **287**, 637–640 (2000).
6. Salvetat, J. P. *et al.* Elastic modulus of ordered and disordered multiwalled carbon nanotubes. *Adv. Mater.* **11**, 161–165 (1999).
7. Shaffer, M. S. P. & Windle, A. H. Fabrication and characterization of carbon nanotube/poly(vinyl alcohol) composites. *Adv. Mater.* **11**, 937–941 (1999).
8. Haggenmueller, R., Gommans, H. H., Rinzler, A. G., Fischer, J. E. & Winey, K. I. Aligned single-wall carbon nanotubes in composites by melt processing methods. *Chem. Phys. Lett.* **330**, 219–225 (2000).
9. Watts, P. C. P. *et al.* A low resistance boron-doped carbon nanotube-polystyrene composite. *J. Mater. Chem.* **11**, 2482–2488 (2001).
10. Vigolo, B. *et al.* Macroscopic fibers and ribbons of oriented carbon nanotubes. *Science* **290**, 1331–1334 (2000).
11. Salvetat, J. P. *et al.* Elastic and shear moduli of single-walled carbon nanotube ropes. *Phys. Rev. Lett.* **82**, 944–947 (1999).
12. Chen, J. *et al.* Dissolution of full-length single-walled carbon nanotubes. *J. Phys. Chem. B* **105**, 2525–2528 (2001).
13. Frankland, S. J. V., Caglar, A., Brenner, D. W. & Griebel, M. Molecular simulation of the influence of chemical crosslinks on the shear strength of carbon nanotube-polymer interfaces. *J. Phys. Chem. B* **106**, 3046–3048 (2002).
14. Star, A. *et al.* Preparation and properties of polymer-wrapped single-walled carbon nanotubes. *Angew. Chem. Int. Edn Engl.* **40**, 1721–1725 (2001).
15. Decher, G. Fuzzy nanoassemblies toward layered polymeric multicomposites. *Science* **277**, 1232–1237 (1997).
16. Wu, A., Yoo, D., Lee, J. K. & Rubner, M. F. Solid-state light-emitting devices based on the tris-chelated ruthenium(II) complex: 3. High efficiency devices via a layer-by-layer molecular-level blending approach. *J. Am. Chem. Soc.* **121**, 4883–4891 (1999).
17. Mamedov, A. A., Belov, A., Giersig, M., Mamedova, N. N. & Kotov, N. A. Nanorainbows. Graded semiconductor films from quantum dots. *J. Am. Chem. Soc.* **123**, 7738–7739 (2001).
18. Mamedov, A. A., Guldi, D. M., Prato, M. & Kotov, N. A. Layer-by-layer assembly of carbon nanotubes. Proceedings of 223rd ACS National Meeting, Orlando, Florida, United States, April 7–11, 2002, COLL-173, ACS, Washington D.C.
19. Rouse, J. H., Ounaies, Z., Lellehei, P. T. & Siochi, E. J. Incorporation of carbon nanotubes within stepwise assembled polyelectrolyte films. Proceedings of 223rd ACS National Meeting, Orlando, Florida, United States, April 7–11, 2002, COLL-169, ACS, Washington D.C.
20. Mamedov, A. A. & Kotov, N. A. Free-standing layer-by-layer assembled films of magnetite nanoparticles. *Langmuir* **16**, 5530–5533 (2000).
21. Mawhinney, D. B. *et al.* Surface defect site density on single walled carbon nanotubes by titration. *Chem. Phys. Lett.* **324**, 213–216 (2000).
22. Rols, S. *et al.* Diameter distribution of single wall carbon nanotubes in nanobundles. *Eur. Phys. J. B* **18**, 201–205 (2000).
23. Westenhoff, S. & Kotov, N. A. Quantum dot on a rope. *J. Am. Chem. Soc.* **124**, 2448–2449 (2002).
24. Sullivan, D. M. & Bruening, M. L. Ultrathin, ion-selective polyimide membranes prepared from layered polyelectrolytes. *J. Am. Chem. Soc.* **123**, 11805–11806 (2001).
25. Li, F., Cheng, H.-M., Bai, S., Su, G. & Dresselhaus, M. S. Tensile strength of single-walled carbon nanotubes directly measured from their macroscopic ropes. *Appl. Phys. Lett.* **77**, 3161–3163 (2000).
26. Thompson, J. B. *et al.* Bone indentation recovery time correlates with bond reforming time. *Nature* **414**, 773–776 (2001).
27. Smith, B. L. *et al.* Molecular mechanistic origin of the toughness of natural adhesives, fibres and composites. *Nature* **399**, 761–763 (1999).
28. *CRC Materials Science and Engineering Handbook* (CRC, Boca Raton, Florida, USA, 1992).
29. Fu, S. Y. *et al.* Hybrid effects on tensile properties of hybrid short-glass-fiber- and short-carbon-fiber-reinforced polypropylene composites. *J. Mater. Sci.* **36**, 1243–1251 (2001).
30. Yu, M. F., Files, B. S., Arepalli, S. & Ruoff, R. S. Tensile loading of ropes of single wall carbon nanotubes and their mechanical properties. *Phys. Rev. Lett.* **84**, 5552–5555 (2000).
31. Garg, A. & Sinnott, S. B. Effect of chemical functionalization on the mechanical properties of carbon nanotubes. *Chem. Phys. Lett.* **295**, 273–278 (1998).

Molecular design of strong single-wall carbon nanotube/polyelectrolyte multilayer composites

ARIF A. MAMEDOV, NICHOLAS A. KOTOV, MAURIZIO PRATO, DIRK M. GULDI, JAMES P. WICKSTED AND ANDREAS HIRSCH

Nature Materials **1**, 190–194 (2002).

In this article, the manufacture of SWNTs was incorrectly described in lines 18 and 19 of the second column on page 191. It should have read as follows:
The SWNTs were manufactured by laser vaporization of carbon rods, which were doped with Co/Ni in a 1:1 ratio in an atmosphere of Ar.

An additional statement should also have appeared in the Acknowledgements section as follows:
The SWNTs used in this work were supplied by M. Kappes and F. Hennrich (University of Karlsruhe, Germany).